FORECASTERS' FORUM

Examination of the Predictability of Nocturnal Tornado Events in the Southeastern United States

RYAN C. BUNKER,[a,g] ARIEL E. COHEN,[b,h] JOHN A. HART,[c] ALAN E. GERARD,[d]
KIM E. KLOCKOW-MCCLAIN,[e] AND DAVID P. NOWICKI[f,i]

[a] *Center for Analysis and Prediction of Storms National Weather Center Research Experiences for Undergraduates Program, and University of Oklahoma, Norman, Oklahoma*
[b] *NOAA/NWS/Storm Prediction Center, and School of Meteorology, University of Oklahoma, Norman, Oklahoma*
[c] *NOAA/NWS/Storm Prediction Center, Norman, Oklahoma*
[d] *Warning Research and Development Division/National Severe Storms Laboratory, Norman, Oklahoma*
[e] *Cooperative Institute for Mesoscale Meteorological Studies/National Severe Storms Laboratory, Norman, Oklahoma*
[f] *Center for Analysis and Prediction of Storms National Weather Center Research Experiences for Undergraduates Program, University of Oklahoma, Norman, Oklahoma, and University of Mississippi, Oxford, Mississippi*

ABSTRACT

Tornadoes that occur at night pose particularly dangerous societal risks, and these risks are amplified across the southeastern United States. The purpose of this study is to highlight some of the characteristics distinguishing the convective environment accompanying these events. This is accomplished by building upon previous research that assesses the predictive power of meteorological parameters. In particular, this study uses the Statistical Severe Convective Risk Assessment Model (SSCRAM) to determine how well convective parameters explain tornado potential across the Southeast during the months of November–May and during the 0300–1200 UTC (nocturnal) time frame. This study compares conditional tornado probabilities across the Southeast during November–May nocturnal hours to those probabilities for all other November–May environments across the contiguous United States. This study shows that effective bulk shear, effective storm-relative helicity, and effective-layer significant tornado parameter yield the strongest predictability for the November–May nocturnal Southeast regime among investigated parameters. This study demonstrates that November–May southeastern U.S. nocturnal predictability is generally similar to that within other regimes across the contiguous United States. However, selected ranges of multiple parameters are associated with slightly better predictability for the nocturnal Southeast regime. Additionally, this study assesses conditional November–May nocturnal tornado probabilities across a coastal domain embedded within the Southeast. Nocturnal coastal tornado predictability is shown to generally be lower than the other regimes. All of the differences highlight several forecast challenges, which this study analyzes in detail.

[g] Current affiliation: National Weather Service Forecast Office, Topeka, Kansas and School of Meteorology, University of Oklahoma, Norman, Oklahoma.

[h] Current affiliation: National Weather Service Forecast Office, Miami, Florida.

[i] Current affiliation: University of Mississippi, Oxford, Mississippi.

Corresponding author: Ryan C. Bunker, Ryan.Bunker@noaa.gov

1. Introduction

The overnight hours, defined as 0300–1200 UTC in the present study, represent a time when society is particularly vulnerable to tornadoes. Ashley et al. (2008) found that nocturnal tornadoes are 2.5 times more likely to kill as those that occur during the daytime. The southeastern United States is a region of the country where there exists particularly high societal vulnerability to tornadoes (Ashley 2007; Ashley and Strader 2016)—especially for nocturnal tornadoes (Ashley et al. 2008). Figure 6 from Ashley et al. (2008) highlights portions of the Southeast
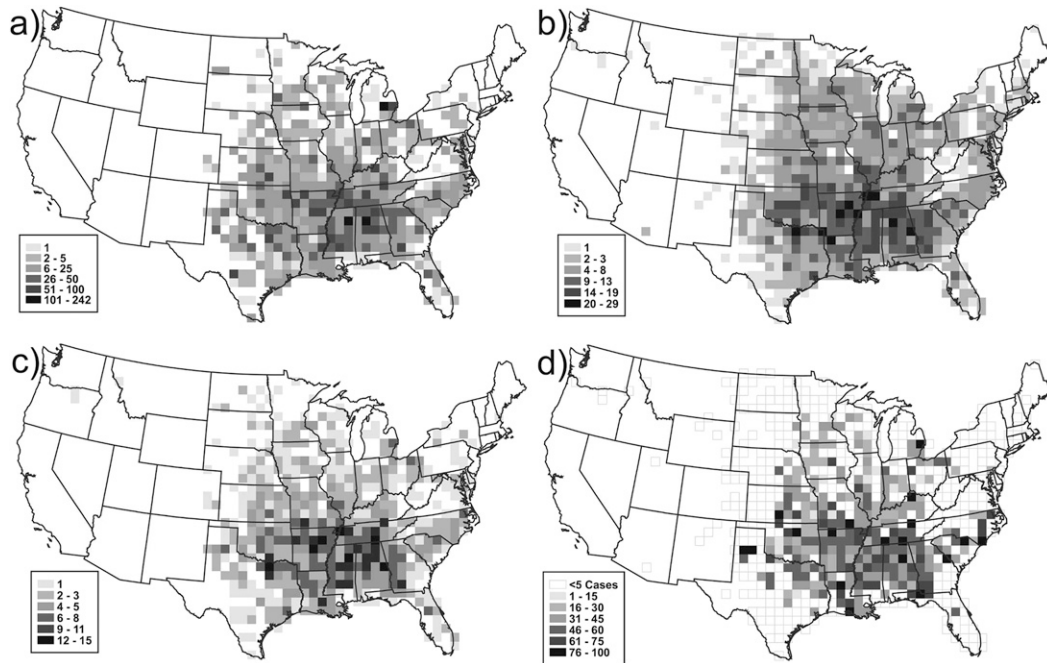
FIG. 1. Figure 7 from Ashley et al. (2008) that illustrates (a) number of nocturnal tornado fatalities, (b) number of killer tornado events, (c) number of *nocturnal* killer tornado events, and (d) percent nocturnal killer events. Open grid cells in (d) indicate that fewer than five killer tornado events occurred from 1880 to 2007.

as seeing the greatest proportion of total tornadoes at night (approximately 30%–40%). Meanwhile, Fig. 7 of Ashley et al. (2008; Fig. 1 in the present work) highlights a corridor from eastern Oklahoma to western Georgia with the highest percent of killer nocturnal tornado events. They specified that an important aspect of this analysis is that the concentration of nocturnal percent killer tornado events is densest across the Southeast, which highlights the nocturnal tornado vulnerability specific to this portion of the country. As an extension, they speculated that this may explain the elevated mortality from tornadoes across this area as noted by Ashley (2007).

Ultimately, the work of Ashley et al. has motivated the need to focus additional research on nocturnal tornadoes in the Southeast. The application of this research could support enhancements to the accuracy and communication of nocturnal tornado forecasts across this part of the country. Also, an analysis of spatiotemporal frequencies of tornado occurrence across the contiguous United States reveals an inland displacement of right-moving supercell significant tornadoes and quasi-linear convective system EF1+ tornadoes from the coast [Figs. 15 and 16 of Thompson et al. (2012)]. This motivates investigation of subregional variability of tornado predictability.

Following the results of Hart and Cohen (2016a), and for all regimes addressed in this work, the present study focuses on tornadoes occurring exclusively during the months of November–May. Hart and Cohen (2016a) found that during the months of November–May, tornadoes are more predictable across the contiguous United States compared to other times of the year, based on the Statistical Severe Convective Risk Assessment Model (SSCRAM; Hart and Cohen 2016b). Also, across the Southeast, tornado frequencies—for right-moving supercell significant tornadoes and quasi-linear convective system EF1+ tornadoes—were found to be maximized during the winter and spring (relative to other times of the year) based on Thompson et al. (2012).

Nighttime tornadoes that occur across the Southeast during the months of November–May are often accompanied by weak buoyancy [represented by the vertically integrated quantity of convective available potential energy (CAPE)], and strong vertical wind shear, as this period of time also encompasses the winter season when both insolation and buoyancy are more typically muted. Low-buoyancy, strong-shear environments have been addressed by numerous studies (e.g., Guyer et al. 2006; Guyer and Dean 2010; Sherburn and Parker 2014; Cohen et al. 2015, 2017). These environments present specific forecast challenges, including those stemming from parameterizing the planetary boundary layer in numerical weather prediction models (e.g., Cohen et al. 2015, 2017). Sherburn and Parker (2014) addressed high-shear, low-CAPE (HSLC) environments in more general terms and provided an assessment of the predictive power of meteorological

variables in these environments. These studies highlight the characteristics of weak-buoyancy environments that can often characterize nocturnal tornado events. Daytime tornado environments typically are associated with larger amounts of buoyancy (Davies and Fischer 2009) associated with stronger heating resulting from insolation. On the other hand, the weaker buoyancy characteristic of nighttime tornado environments inherently renders greater sensitivity of numerical simulations to buoyancy-related parameters such as temperature and mixing ratio (Cohen et al. 2017). Overall, there have been many attempts to improve forecasts of tornadoes through the evaluation of numerical weather prediction model output and conceptual models (e.g., Scofield and Purdom 1986; Lewis 1989; Burgess and Lemon 1990; Galway 1992; Johns and Doswell 1992; Bryan et al. 2003; Schwartz et al. 2014) to distinguish environments potentially capable of producing tornadoes from those that do not.

From the aforementioned work, it is apparent that there is motivation to better understand the predictability of nocturnal tornado environments across the southeastern United States. This challenge has societal implications and is exacerbated by the weak-buoyancy characteristic of the nocturnal environments. The subsequent focus of the present study is to consider these three problems in more detail, and address the following questions: How predictable are tornadoes across the Southeast at night? How does this predictability change when considering exclusively the coastal areas? This study aims to address this question by investigating a selection of convective parameters to reveal behaviors of nocturnal Southeast tornado predictability. This is accomplished by creating conditional probability distributions using SSCRAM (Hart and Cohen 2016b). This work uses conditional probability distributions—created as described in section 2—to illustrate the predictability of November–May Southeast nocturnal tornadoes, as discussed in section 3. Conclusions and a summary are provided in section 4.

2. Methodology

The probabilities discussed in this study are based upon SSCRAM output (Hart and Cohen 2016b) from November to May. SSCRAM output provides the relative frequency of historical severe weather events occurring 2 h into the future given environmental parameters and the presence of cloud-to-ground lightning; it effectively uses diagnostic parameters to draw conclusions about the future impacts. The way in which SSCRAM is designed and operates is illustrated in detail in Fig. 2 (reproduced from Hart and Cohen 2016b). Figure 2 also highlights the process by which severe weather reports are gathered.

SSCRAM identifies all 40-km Rapid Update Cycle (RUC) model/Rapid Refresh (RAP) model grid boxes in which cloud-to-ground (CG) lightning occurs. Within these grid boxes in which lightning occurs, several attributes are also documented, such as the date, time, center point of the grid box (latitude/longitude), and environmental conditions from the SPC mesoanalysis system (Bothwell et al. 2002) characteristic of the near-storm environment for that grid box. A storm trajectory is determined for each grid box for the 2 h subsequent to the hour in which lightning occurred in the grid, based on the Bunkers et al. (2000) right-moving supercell motion. Then, 40-km-radius search areas are identified surrounding points along the assumed storm trajectory, from which any severe weather reports are gathered. By comparing the total number of grid boxes in which lightning occurred within 2 h after CG lightning occurred—which includes those grid boxes associated with tornado reports and those not associated with tornado reports (null events)—to the total number grid boxes that were associated with tornado occurrences, conditional tornado probabilities are derived. These probabilities are conditional upon CG lightning occurrence.

For example, a conditional probability of 40% for a particular parameter range signifies that 40% of lightning-producing convective elements within that parameter range are associated with a downstream tornado report within the next 2 h. This process is repeated for various ranges of parameter values to generate conditional probability distributions. The definition of "good" predictability herein follows the description provided by Hart and Cohen (2016a,b)—conditional probability distributions that exhibit appreciable change over a diverse range of convective parameter values.

Hart and Cohen (2016b) addressed the lack of explicit accounting for convective morphology in SSCRAM; SSCRAM is intended to provide consistent, reproducible statistical guidance regarding severe threats from any convective mode without incorporation of the subjectivity of convective-mode assessment. However, they do identify the validity of the use of search radii surrounding points accompanying the right-moving supercell motion vector as best representing convective motions that account for severe storm report occurrences. Also, one limitation of the present work is that it does not account for tornado-producing environments that fail to produce CG lightning. Guyer and Dean (2015) provided a thorough analysis of tornado environments in which CG lightning did not occur and indicate the small magnitude of buoyancy that characterize them (mixed-layer CAPE below $500 \, \mathrm{J \, kg^{-1}}$ for 82% of cases in their dataset]. Despite the known existence of non-lightning-producing, tornadic convection, Guyer and Dean (2015) acknowledged that they are relatively rare,
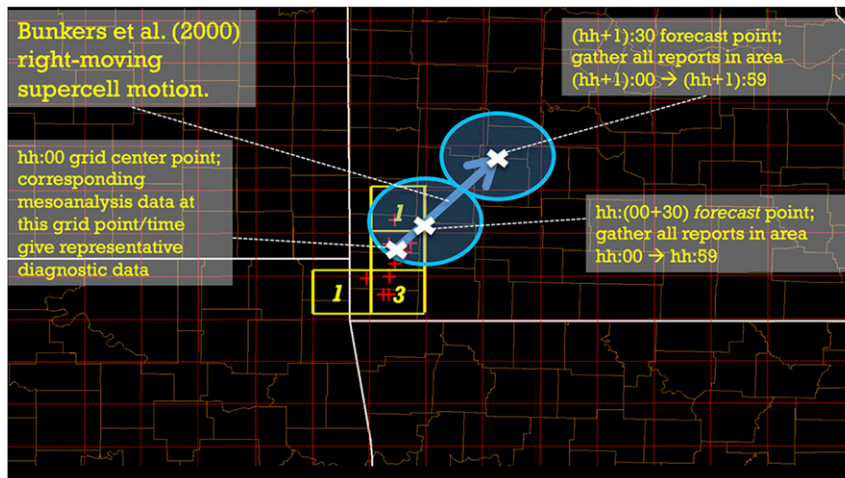
FIG. 2. Figure 1 from Hart and Cohen (2016b) that illustrates the design of SSCRAM, by which downstream severe storm reports are queried within a defined space and time emanating from each grid box associated with lightning. Two different search areas are determined by extrapolation from the center of the grid associated with lightning, using an assumed forward projection along a right-moving supercell motion vector from Bunkers et al. (2000). Each search area is represented by a circle outline with radius of 40 km, with the total search duration spanning 2 h of severe storm reports subsequent to lightning occurring in the grid box. Within each search area, severe storm reports are documented if they occur within 30 min of the time corresponding to the forward-extrapolated point.

with a total of only 293 documented tornadoes from 2005 to 2014 being associated with no CG lightning. This represents a very small proportion of the total tornado count during this time period (Guyer and Dean 2015), which does not present a major problem in identifying more substantial signals of predictability for tornadoes in the context of SSCRAM.

Using SSCRAM, environmental parameters considered in this study include 0–1-km bulk shear, 0–1-km storm-relative helicity (SRH), 100-mb mixed-layer CAPE (MLCAPE; 1 mb = 1 hPa), 100-mb mixed-layer lifted condensation level (MLLCL) heights, effective bulk shear, effective storm-relative helicity (effective SRH), and effective-layer significant tornado parameter (STP). This set of parameters represents necessary conditions favoring organized severe convection (i.e., moisture, lift, instability, and vertical wind shear) in a bulk sense (Schaefer 1986), without substantial redundancies of environmental conditions among the studied parameters. The formulations for the effective parameters are defined by Thompson et al. (2007, 2012).

In this study, November–May data are collected from SSCRAM for three separate regimes, for the months of November–May from 2006 to 2015 and between 0300 and 1200 UTC (the nocturnal hours). One regime encompasses lightning-producing environments that occur during the nocturnal hours across a southeastern United States domain (outlined in Fig. 3), hereafter referenced as "SE_noc." To compare this unique dataset with

all other lightning-producing environments occurring across the contiguous United States, a second regime is studied (i.e., consisting of lightning-producing environments across the Southeast during nonnocturnal hours and any time outside of the Southeast (across the remainder of the contiguous United States)]. This second regime is hereafter be referenced as "non-SE_noc," which effectively encompasses the characteristics of all contiguous U.S. environments outside of the SE_noc regime, to provide a holistic dataset for comparison. This holistic comparison permits a robust sample to which the SE_noc regime is compared—accounting more completely for both geographic and temporal differences. Finally, a third regime is investigated [i.e., nocturnal lightning-producing environments across a coastal domain embedded within the Southeast (Fig. 3), which is hereafter referenced as "Coastal_noc"]. SSCRAM data for the SE_noc and Coastal_noc regimes are compared to those from the non-SE_noc regime. This means that there is overlap between the SE_noc and Coastal_noc regimes, but no mutual overlap exists between the non-SE_noc regime and either the SE_noc or Coastal_noc regimes.

Differences between SE_noc tornado predictability and non-SE_noc tornado predictability are investigated, and also tornado predictability within the Coastal_noc regime is compared to that within the non-SE_noc regime. These differences will be tested by creating conditional probability distribution plots for different parameters and evaluating statistical significance between distributions.
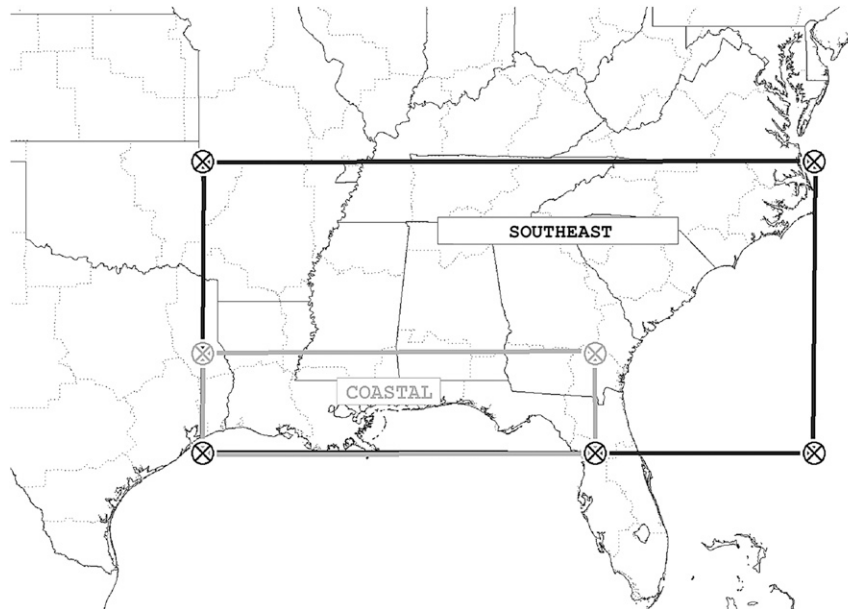
FIG. 3. Map of study domains. The regime of nocturnal environments occurring within the domain labeled "SOUTHEAST" (black outline) is referenced as "SE_noc", the regime encompassing all other environments across the contiguous United States is referenced as "non-SE_noc", and the regime of environments occurring within the subdomain labeled "COASTAL" (gray outline) embedded within the broader "SOUTHEAST" domain is referenced as "Coastal_noc". Outlines of National Weather Service County Warning Areas are indicated by dotted lines.

The subsequent statistical analysis is illustrated in terms of 1) plotted distributions of conditional probabilities of tornadic events, as described by Hart and Cohen (2016b); and 2) evaluation of the statistical significance of the differences between the SE_noc and non-SE_noc regimes, and between the Coastal_noc and non-SE_noc regimes.

Statistical significance is evaluated using a two-tailed Z test comparing two proportions, and corresponding p values (Devore 2015) were computed to determine whether differences between distributions are statistically significant. These p values are graphically depicted and are interpreted as follows: a p value of <0.05 indicates that the difference between the two compared regimes for a given parameter range is statistically significant, and a p value of 0.05–0.10 indicates that the difference between the two compared regimes for a given parameter range is *marginally* statistically significant. To remain consistent with Hart and Cohen (2016a,b), the number of environments must be 25 or greater for consideration in this study.

3. Results and discussion

a. Southeast domain versus outside Southeast domain

One example of a predictor of tornadoes is effective bulk shear (Fig. 4). Using effective bulk shear, the predictability of tornadoes in the SE_noc regime is generally similar to that within the non-SE_noc regime, though the SE_noc regime is associated with slightly better predictability for effective bulk shear from 45 to 70 kt (1 kt $\approx$ 0.51 m s^{-1}). Differences between the SE_noc and non-SE_noc regime are statistically significant from 65 to 75 kt. The conditional probability minimum at 75–80 kt of effective shear could be explained by a sharp drop-off in the sample size of environments with effective shear above 75 kt, similar to some of the behaviors of small-sample-size portions of the distributions identified by Hart and Cohen (2016b). In a similar manner, both effective SRH and STP offer predictability for SE_noc tornadoes—similar to tornadoes within the non-SE_noc regime (Figs. 5 and 6, respectively). For example, conditional probabilities for both STP and effective SRH increase from the lower single digits to the 20s (percent) over the ranges of parameter values, with similar to slightly stronger positive slopes for SE_noc distributions compared to non-SE_noc distributions.

Unlike effective shear, effective SRH, and STP, the conditional probabilities of tornado events for the SE_noc regime are found to increase only slightly with increasing 0–1-km bulk shear (Fig. 7). This suggests that the overall utility of 0–1-km shear in predicting tornadoes is only modest for the SE_noc regime, as it is for
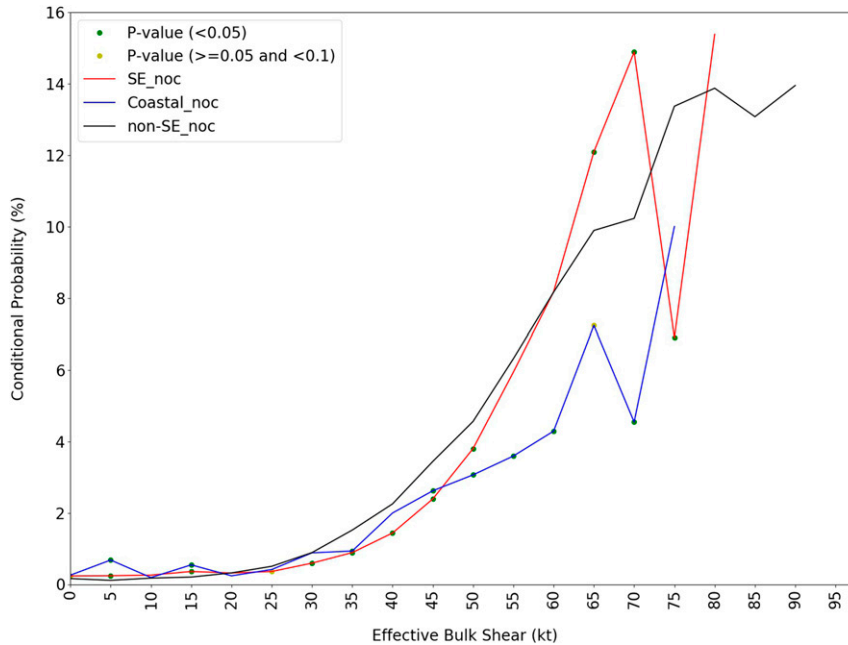
FIG. 4. Conditional tornado probability distribution for the SE_noc regime (red), non-SE_noc regime (black), and Coastal_noc regime (blue) for effective bulk shear. The x-axis labels provide the lower limit of each incremental effective shear magnitude range. The p values representing statistically significant different conditional probabilities between the SE_noc and non-SE_noc regimes, and between the Coastal_noc and the non-SE_noc regimes, are depicted by small dots overlaid on the conditional probability distributions for the Southeast domain, and the coastal domain, respectively. Statistically significant differences (p values below 0.05) are represented by green dots, and marginally statistically significant differences (p values at least 0.05 but below 0.10) are represented by yellow dots.

non-SE_noc. However, for a confined range of 30–45 kt of 0–1-km bulk shear, SE_noc tornado predictability is slightly better than that for non-SE_noc, with probability differences being statistically significant below 40 kt. Similar to 0–1-km bulk shear, 0–1-km SRH conveys a similar pattern regarding nocturnal tornado predictability (Fig. 8). The overall predictability is quite weak, reaching a maximum probability of only 6%. However, for a confined range of 200–400 $m^2 s^{-2}$ of 0–1-km SRH, SE_noc tornado predictability is slightly better than that for non-SE_noc, with probability differences between the two regimes being statistically significant at selected parameter ranges.

Similarly, conditional probabilities of tornado events do not vary substantially with differences in MLCAPE for SE_noc (Fig. 9). This suggests that MLCAPE does not explain variations in tornado predictability well for SE_noc—rendering limitations to its use in SE_noc tornado threat assessment, similar to non-SE_noc. However, for MLCAPE at or below 1250 J kg^{-1}, actual SE_noc tornado probabilities are slightly higher in magnitude than non-SE_noc tornado probabilities, and these differences are statistically significant. While conditional

probabilities for tornadoes are found to decrease for increasing MLCAPE above 1500 J kg^{-1} with variable levels of statistical significance, this may reflect the reduction in sample sizes for MLCAPE increasing above 1500 J kg^{-1}. Compared to 83 558 total SE_noc lightning-producing environments with MLCAPE below 1500 J kg^{-1}, only 3165 (311) SE_noc lightning-producing environments contain MLCAPE at least 1500 J kg^{-1} (2500 J kg^{-1}) within the parameter ranges represented by the x axis in Fig. 9.

The lack of predictability exhibited by MLCAPE can be explained by the relative importance of other environmental parameters to the tornado risk in these typical low-buoyancy environments (e.g., deep shear). Cohen et al. (2017) identified systematic errors in buoyancy calculations from reconstructed soundings similar to the input for the SPC mesoanalysis system in low-buoyancy, strong wind shear environments when compared to observed soundings (i.e., a low-buoyancy bias). This error has the potential to extend to the muted predictability based on buoyancy, for which Cohen et al. (2017) identified as a substantially sensitive factor in typifying weak-buoyancy environments. However, given
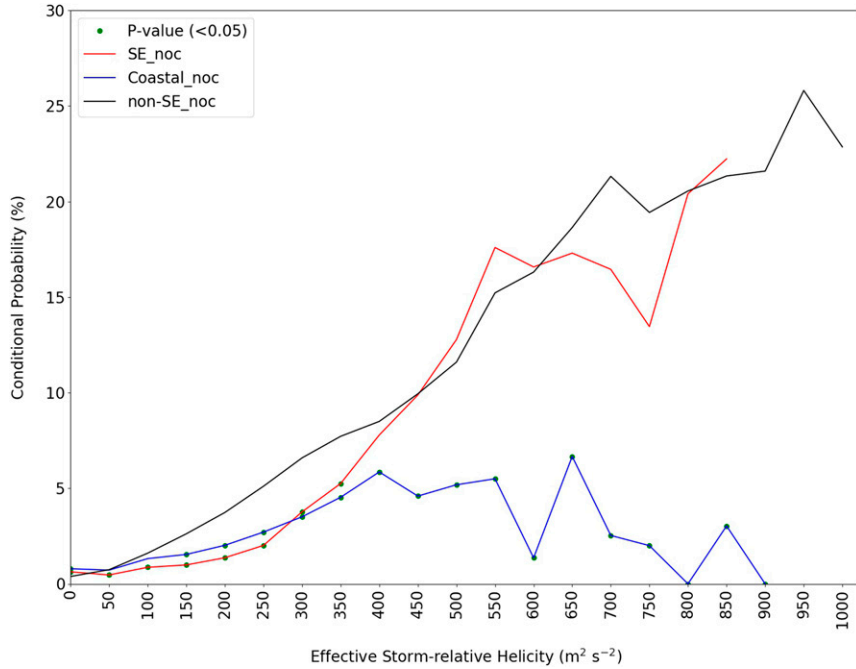
FIG. 5. As in Fig. 4, but for effective storm-relative helicity and a *y* axis from 0% to 30%.

that this is an established bias for the mesoanalysis system that serves as a benchmark for convective environment analysis—which also serves as a basis for SSCRAM input—there is indeed repeatability in errors; knowledge of these errors can serve to alleviate

unexpected assertions regarding tornado predictability. Additionally, the influence of MLCAPE on STP could provide some explanation for the lower tornado probabilities (based on STP) for the SE_noc regime compared to the non-SE_noc regime. However, the slope of
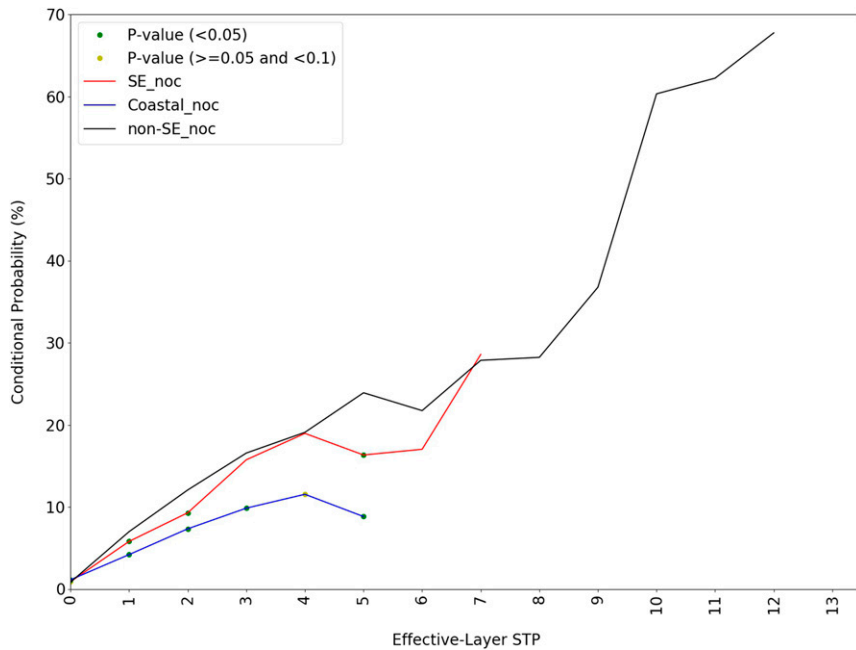
FIG. 6. As in Fig. 4, but for effective-layer significant tornado parameter and a *y* axis from 0% to 70%.
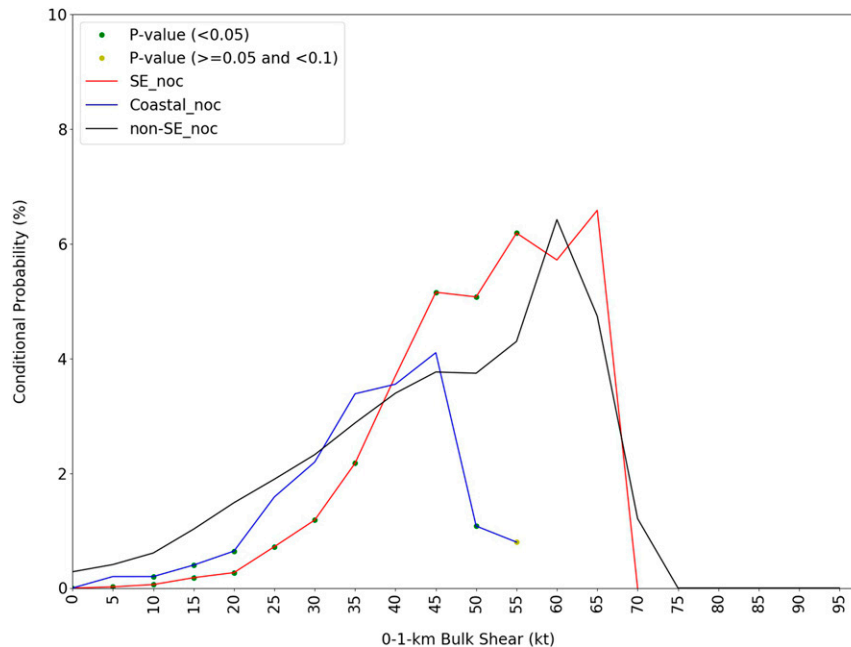
FIG. 7. As in Fig. 4, but for 0–1-km bulk shear and a *y* axis from 0% to 10%.

the STP-based probability distribution for the SE_noc regime is similar to that for the non-SE_noc regime, suggesting similar tornado predictability between these regimes using STP.

Similarly, for another thermodynamic variable—MLLCL—predictability within the SE_noc regime is limited, as it is for non-SE_noc (Fig. 10). Hart and Cohen (2016b) addressed the limited utility of MLLCL in tornado predictability. Specifically, they found that an overwhelming number of environments supporting organized, surface-based convection fail to produce tornadoes regardless of the MLLCL, with little change in conditional tornado probabilities resulting from changes in MLLCL. They found that the predictability of tornadoes is much greater when considering effective SRH. Overall, Figs. 9 and 10 suggest that the predictability of nocturnal tornadoes based on thermodynamic variables investigated in the present work is similar among all three regimes: SE_noc, Coastal_noc, and non-SE_noc (except for MLCAPE, which could be explained by small sample sizes within the Southeast domain for higher magnitudes of MLCAPE).

b. Coastal domain versus outside Southeast domain

To illustrate variations in nocturnal predictability within the SE_noc regime, parameters within the Coastal_noc regime are also examined to investigate subregional predictability within the SE_noc regime. Figures 4–6 suggest a common tendency for the Coastal_noc regime to exhibit significantly lower probabilities

than non-SE_noc tornadoes and even lower probabilities than SE_noc tornadoes for multiple parameter ranges. These factors highlight that the nocturnal tornado predictability varies within the SE_noc regime, with Coastal_noc tornadoes generally being associated with less predictability than SE_noc tornadoes. Some of this relatively reduced predictability could be related to the comparatively lower sample sizes of Coastal_noc lightning-producing environments. However, as an example, for effective SRH of 350–650 $m^2 s^{-2}$, Coastal_noc tornado probabilities are consistently lower in magnitude (with a general smaller distribution slope) than SE_noc and non-SE_noc tornado probabilities, despite over 100 Coastal_noc lightning-producing environments documented for each parameter range bin. Similarly, for effective-layer STP from 1 to 4, Coastal_noc tornado probabilities are less (with a general smaller distribution slope) than the two other comparison regimes, yet sample sizes of at least 75 Coastal_noc lightning-producing environments were documented for each parameter range bin.

We seek to informally investigate the differences in nocturnal tornado predictability between the Coastal_noc regime and the SE_noc regime, and more in-depth analyses of nocturnal tornado predictability within the SE_noc regime could be the focus of subsequent research. Figure 11 highlights the large-scale patterns characteristic of nocturnal tornadoes for a pair of cases across the Southeast. In both of these cases, a well-defined plume of moist air characterized by 60°F surface dewpoints
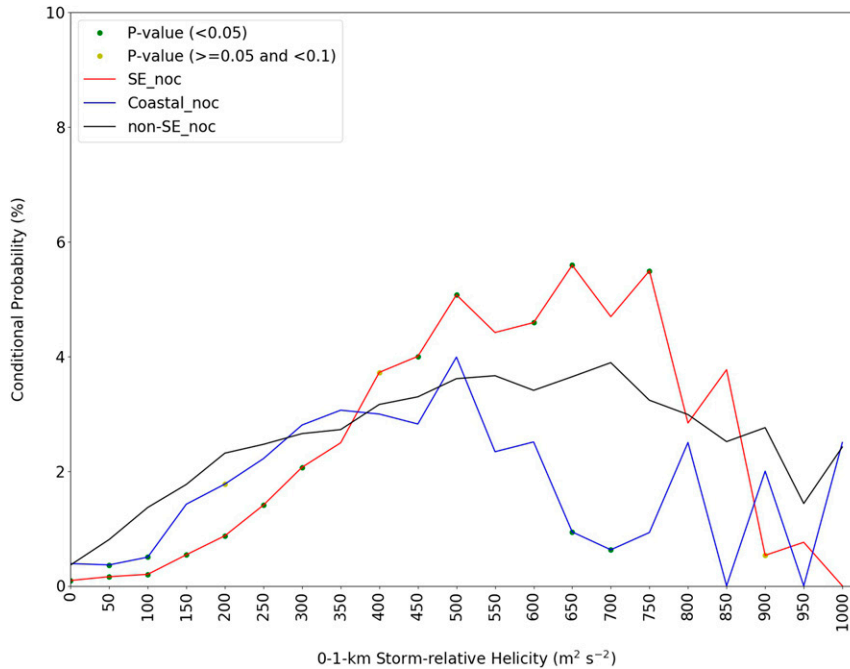
FIG. 8. As in Fig. 4, but for 0–1-km storm-relative helicity and a *y* axis from 0% to 10%.

emanating from the Gulf of Mexico extends inland within the warm sector of an extratropical cyclone centered well north of the richest moisture. In both of these cases, the most favorable moisture content was displaced well to the south of stronger deep ascent implied

by the location of the extratropical cyclone. Composite radar loops (not shown) for both of these cases indicate that the initial convective cells in these cases originated over the coastal domain in proximity to the richest moisture. This initial convection was steered northward
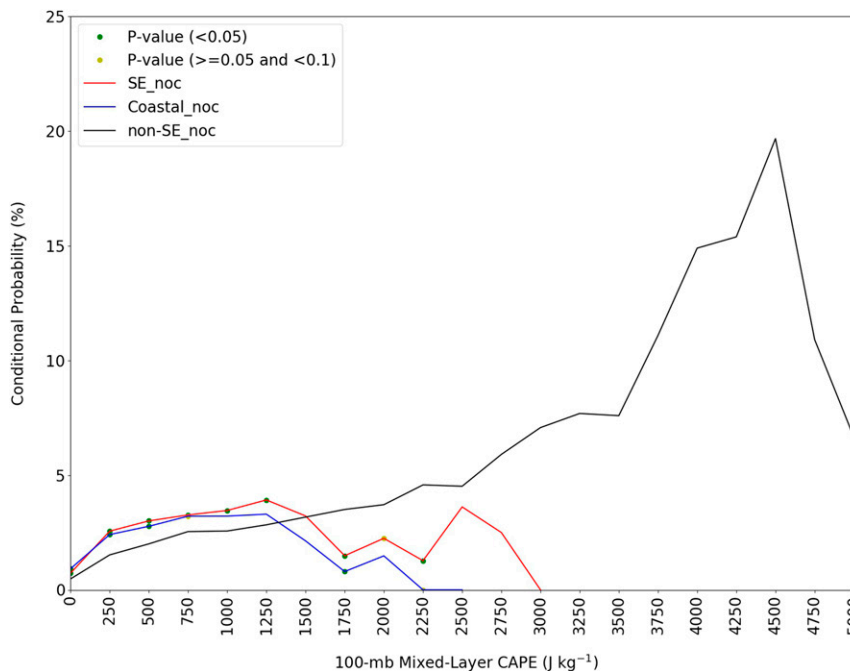
FIG. 9. As in Fig. 4, but for MLCAPE and a *y* axis from 0% to 25%.
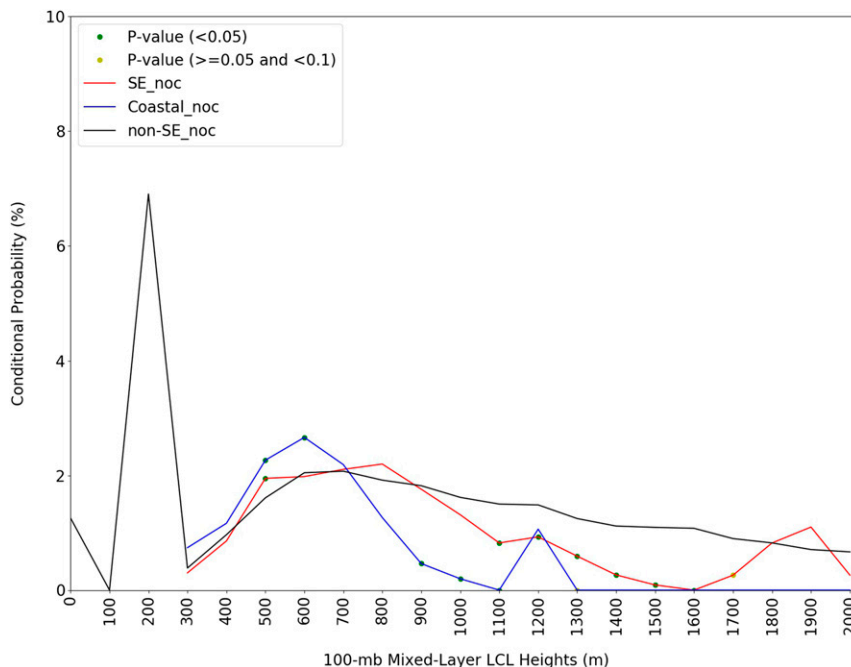
FIG. 10. As in Fig. 4, but for lowest-100-mb mixed-layer LCL heights and a *y* axis from 0% to 10%.

in concert with the poleward low-level mass flux accompanying the larger-scale cyclone, while experiencing intensification north of the coastal domain (the geographic area encompassing the Coastal_noc regime). In both of these cases, tornadic-storm-favoring thermodynamic and kinematic profiles existed over a broad portion of the Southeast domain (the geographic area encompassing the SE_noc regime). However, forcing for ascent accompanying the larger-scale cyclone governed locations of convective development and intensification, which may explain the relatively muted nocturnal tornado predictability within the Coastal_noc regime associated with climatologically favored patterns of Northern Hemisphere cyclone tracks (e.g., Rudeva and Gulev 2007). In both of these cases, the muted predictability of tornadoes within the Coastal_noc regime could be associated with its location being the focus for initiation of convective storms that subsequently produced tornadoes elsewhere within the Southeast domain, and this could be typical of other similar regimes. The use of SSCRAM for depicting the evolution of tornado probabilities during a convective event in these types of regimes could be a focus of subsequent research.

4. Conclusions

This work uses the Statistical Severe Convective Risk Assessment Model (SSCRAM; Hart and Cohen 2016b)

to evaluate the predictability of nocturnal tornadoes using convective parameters across the southeastern United States during the months of November–May. These months tend to be associated with stronger predictability of significant tornadoes across the contiguous United States (Hart and Cohen 2016a) and are most likely to offer an operationally relevant signal. Effective bulk shear, effective SRH, and effective-layer STP were all found to offer the strongest predictability of nocturnal Southeast tornadoes. The predictability of Southeast nocturnal tornadoes using these parameters is generally similar to the predictability of tornadoes occurring in all other regimes across the contiguous United States. On the other hand, MLCAPE, MLLCL, 0–1-km bulk shear, and 0–1-km SRH provide more muted predictability of nocturnal Southeast tornadoes. However, embedded parameter ranges of multiple parameters are associated with comparatively slightly better tornado predictability for the Southeast nocturnal regime.

Another critical finding is that nocturnal tornado predictability within the coastal domain is associated with markedly weaker tornado predictability compared to environments outside of the nocturnal Southeast regime. Several parameter ranges offer significantly smaller conditional probabilities of nocturnal tornado occurrence for the coastal region compared to environments outside of the nocturnal Southeast regime. This is a consistent signal across the parameters considered in the present work.
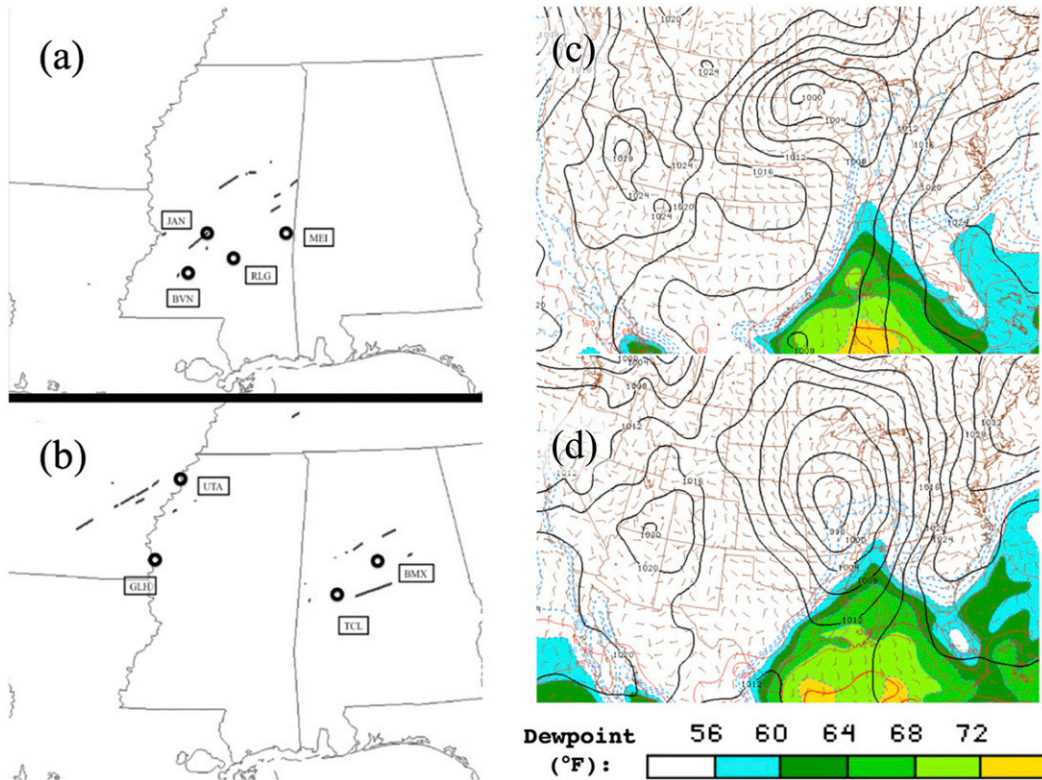
FIG. 11. (left) Combination of Fig. 5 from Cohen et al. (2015) and (right) Fig. 6 of Cohen et al. (2015). Tornado paths marked as black segments from (a) 1200 UTC 31 Dec 2010 to 1200 UTC 1 Jan 2011 and (b) from 1200 UTC 22 Jan to 1200 UTC 23 Jan 2012 (Storm Prediction Center 2013a). Black ovals indicate locations of sounding analyses addressed by Cohen et al. (2015) with city identifiers listed beside the ovals [Jackson (JAN), Brookhaven (BVN), Raleigh (RLG), Meridian (MEI), Greenville (GLH), Tunica (UTA), Tuscaloosa (TCL), and Birmingham (BMX)]. (c),(d) Information pertaining to the mesoscale environment corresponding to (a) and (b), respectively; meso-analysis output (Storm Prediction Center 2013b) based on surface objective analysis (Bothwell et al. 2002) at 0400 UTC 1 Jan 2011 in (c) and 0600 UTC 23 Jan 2012 in (d) for mean sea level pressure (mb; black contours with 4-mb interval), surface isotherms [°F equivalent to (1.8°C + 32); red contours with 5°F interval], surface isodrosotherms [°F equivalent to (1.8°C + 32); dashed contours with 4°F interval and color fill indicating dewpoint values ≥ 56°F], and surface winds [m s^{-1}; barbs with full wind barbs corresponding to 5 m s^{-1} (10 kt) and half barbs to 2.5 m s^{-1}].

A major implication of these findings is that the coastal region of the Southeast is associated with lower predictability of nocturnal tornadoes than other regimes. This highlights the geographically varying nature of the predictability of this high-impact weather.

Collectively, the results of this work are intended to provide operational meteorologists with a framework for quantifying the predictability of a very dangerous phenomenon—nocturnal Southeast U.S. tornadoes—to which society is particularly vulnerable. One commonality among the parameters examined in this work is that conditional probabilities for Southeast nocturnal tornadoes rarely rise above the middle-20-percent range. While these probabilities may seem much lower than those which would offer otherwise greater confidence in the threat of a particular hazard, these conditional probabilities are similar to the maximum probabilities

that Hart and Cohen (2016b) identified with SSCRAM as producing for severe weather hazards for the parameters supporting the greatest predictability (e.g., effective SRH and effective-layer STP yield conditional tornado probabilities no higher than the upper teens to the 20s among all parameter ranges). Some parameters in the present work are found to offer better predictability than others, and behaviors of this predictability vary from parameter to parameter and even within parameter regions and within the Southeast domain. Future work could more formally evaluate the bulk statistical properties of this predictability, through computations of a Brier score for instance, which would involve comparing SSCRAM output from a trained dataset to actual relative frequencies of tornadoes in an independent dataset. Some bulk summary statistics could mask the intricate variability of the parameter-based probability

distributions demonstrated in the present work, and this variability can be critical for a forecaster to perform an accurate severe weather threat assessment based on recognition of the evolving environment. Nevertheless, a more robust evaluation of the SSCRAM output for the Southeast U.S. nocturnal tornado regime could be a focus of future research, though it is outside the scope of identifying predictability as defined in the present work as being a function of the conditional probability distribution.

The findings from this work could serve as guidance to forecasters in providing more accurate forecasts and warnings to protect life and property. Moreover, the application of SSCRAM to quantifying a specific regime of tornado predictability has been demonstrated throughout this work, with this quantification potentially serving as the grounds for incorporation into warn-on-forecast (Stensrud et al. 2009) and Forecasting A Continuum of Environmental Threats (FACETs; Rothfusz et al. 2018) initiatives.

REFERENCES

Ashley, W. S., 2007: Spatial and temporal analysis of tornado fatalities in the United States: 1880–2005. *Wea. Forecasting*, **22**, 1214–1228, https://doi.org/10.1175/2007WAF2007004.1.

——, and S. M. Strader, 2016: Recipe for disaster: How the dynamic ingredients of risk and exposure are changing the tornado disaster landscape. *Bull. Amer. Meteor. Soc.*, **97**, 767–786, https://doi.org/10.1175/BAMS-D-15-00150.1.

——, A. J. Krmenec, and R. Schwantes, 2008: Vulnerability due to nocturnal tornadoes. *Wea. Forecasting*, **23**, 795–807, https://doi.org/10.1175/2008WAF2222132.1.

Bothwell, P. D., J. A. Hart, and R. L. Thompson, 2002: An integrated three-dimensional objective analysis scheme in use at the Storm Prediction Center. Preprints, *21st Conf. on Severe Local Storms*, San Antonio, TX, Amer. Meteor. Soc., J117–J120.

Bryan, G. H., J. C. Wyngaard, and J. M. Fritsch, 2003: Resolution requirements for the simulation of deep moist convection. *Mon. Wea. Rev.*, **131**, 2394–2416, https://doi.org/10.1175/1520-0493(2003)131<2394:RRFTSO>2.0.CO;2.

Bunkers, M. J., B. A. Klimowski, J. W. Zeitler, R. L. Thompson, and M. L. Weisman, 2000: Predicting supercell motion using a new hodograph technique. *Wea. Forecasting*, **15**, 61–79, https://doi.org/10.1175/1520-0434(2000)015<0061:PSMUAN>2.0.CO;2.

Burgess, D. W., and L. R. Lemon, 1990: Severe thunderstorm detection by radar. *Radar in Meteorology,* D. Atlas, Ed., Amer. Meteor. Soc., 619–647.

Cohen, A. E., S. M. Cavallo, M. C. Coniglio, and H. E. Brooks, 2015: A review of planetary boundary layer parameterization schemes and their sensitivity in simulating southeastern U.S. cold season severe weather environments. *Wea. Forecasting*, **30**, 591–612, https://doi.org/10.1175/WAF-D-14-00105.1.

——, ——, ——, ——, and I. L. Jirak, 2017: Evaluation of multiple planetary boundary layer parameterization schemes in southeast United States cold season severe thunderstorm environments. *Wea. Forecasting*, **32**, 1857–1884, https://doi.org/10.1175/WAF-D-16-0193.1.

Davies, J. M., and A. Fischer, 2009: Environmental characteristics associated with nighttime tornadoes. *Electron. J. Oper. Meteor.*, **10** (3), http://nwafiles.nwas.org/ej/pdf/2009-EJ3.pdf.].

Devore, J. L., 2015: *Probability and Statistics for Engineering and the Sciences.* 9th ed. Cengage Learning, 768 pp.

Galway, J. O., 1992: Early severe thunderstorm forecasting and research by the United States Weather Bureau. *Wea. Forecasting*, **7**, 564–587, https://doi.org/10.1175/1520-0434(1992)007<0564:ESTFAR>2.0.CO;2.

Guyer, J. L., and A. R. Dean, 2010: Tornadoes within weak CAPE environments across the continental United States. *25th Conf. on Severe Local Storms,* Denver, CO, Amer. Meteor. Soc., 1.5, https://ams.confex.com/ams/25SLS/techprogram/paper_175725.htm.

——, and ——, 2015: Tornadoes associated with an absence of cloud-to-ground lightning. Extended Abstract, *40th National Weather Association Annual Meeting*, Oklahoma City, OK, NWA, AP-26.

——, A. Kis, K. Venable, and D. A. Imy, 2006: Cool season significant (F2–F5) tornadoes in the Gulf Coast states. *23rd Conf. on Severe Local Storms*, St. Louis, MO, Amer. Meteor. Soc., 4.2, https://ams.confex.com/ams/23SLS/techprogram/paper_115320.htm.

Hart, J. A., and A. E. Cohen, 2016a: The challenge of forecasting significant tornadoes from June to October using convective parameters. *Wea. Forecasting*, **31**, 2075–2084, https://doi.org/10.1175/WAF-D-16-0005.1.

——, and ——, 2016b: The statistical severe convective risk assessment model. *Wea. Forecasting*, **31**, 1697–1714, https://doi.org/10.1175/WAF-D-16-0004.1.

Johns, R. H., and C. A. Doswell, 1992: Severe local storms forecasting. *Wea. Forecasting*, **7**, 588–612, https://doi.org/10.1175/1520-0434(1992)007<0588:SLSF>2.0.CO;2.

Lewis, J., 1989: Real time lightning data and its application in forecasting convective activity. Preprints, *12th Conf. on Weather Analysis and Forecasting,* Monterey, CA, Amer. Meteor. Soc., 97–102.

Rothfusz, L. P., R. Schneider, D. Novak, K. Klockow-McClain, A. E. Gerard, C. Karstens, G. J. Stumpf, and T. M. Smith, 2018: FACETs: A proposed next-generation paradigm for high-impact weather forecasting. *Bull. Amer. Meteor. Soc.*, **99**, 2025–2043, https://doi.org/10.1175/BAMS-D-16-0100.1.

Rudeva, I., and S. K. Gulev, 2007: Climatology of cyclone size characteristics and their changes during the cyclone life cycle. *Mon. Wea. Rev.*, **135**, 2568–2587, https://doi.org/10.1175/MWR3420.1.

Schaefer, J. T., 1986: Severe thunderstorm forecasting: A historical perspective. *Wea. Forecasting*, **1**, 164–189, https://doi.org/10.1175/1520-0434(1986)001<0164:STFAHP>2.0.CO;2.

Schwartz, C. S., G. S. Romine, K. R. Smith, and M. L. Weisman, 2014: Characterizing and optimizing precipitation forecasts from a convection-permitting ensemble initialized by a mesoscale ensemble Kalman filter. *Wea. Forecasting*, **29**, 1295–1318, https://doi.org/10.1175/WAF-D-13-00145.1.

Scofield, R. A., and J. F. W. Purdom, 1986: The use of satellite data for mesoscale analyses and forecasting applications. *Mesoscale Meteorology and Forecasting,* P. S. Ray, Ed., Amer. Meteor. Soc., 118–150.

Sherburn, K. D., and M. D. Parker, 2014: Climatology and ingredients of significant severe convection in high-shear, low-CAPE environments. *Wea. Forecasting*, **29**, 854–877, https://doi.org/10.1175/WAF-D-13-00041.1.

Stensrud, D. J., and Coauthors, 2009: Convective-scale warn-on forecast system: A vision for 2020. *Bull. Amer. Meteor. Soc.*, **90**, 1487–1499, https://doi.org/10.1175/2009BAMS2795.1.

Storm Prediction Center, 2013a: Storm Prediction Center National Severe Weather database browser: Online SeverePlot 3.0. NOAA, accessed 20 September 2013, http://www.spc.noaa.gov/climo/online/sp3/plot.php.

——, 2013b: SPC hourly mesoscale analysis. NOAA, accessed 4 October 2013, http://www.spc.noaa.gov/exper/ma_archive/.

Thompson, R. L., C. M. Mead, and R. Edwards, 2007: Effective storm-relative helicity and bulk shear in supercell thunderstorm environments. *Wea. Forecasting*, **22**, 102–115, https://doi.org/10.1175/WAF969.1.

——, B. T. Smith, J. S. Grams, A. R. Dean, and C. Broyles, 2012: Convective modes for significant severe thunderstorms in the contiguous United States. Part II: Supercell and QLCS tornado environments. *Wea. Forecasting*, **27**, 1136–1154, https://doi.org/10.1175/WAF-D-11-00116.1.